Chemical and Biological Technologies in Agriculture

RESEARCH

Development of soy protein/sodium alginate nanogel-based cress seed gum hydrogel for oral delivery of curcumin

Saeedeh Shahbazizadeh[1], Sara Naji-Tabasi[1*] and Mostafa Shahidi-Noghabi[2]

Abstract

Background: In order to deliver bioactive compounds with better thermal stability and delayed release characteristics, nanogels can be placed inside a hydrogel network. The aim of the present study was to develop isolated soy protein (ISP)–sodium alginate (SA) nanogel (NG) (0, 10, 15 and 20%)-based cress seed gum (CSG) hydrogel as a delivery system of curcumin (Cur). A systematic study was performed to describe the rheological, thermal, microstructural, antioxidant activity properties, and release kinetic of NG-based hydrogels.

Results: Rheological studies showed participation of 10% NG resulted in more elastic, and compact composite with stable diffusion properties. Complex modulus of 10% NG composite was 60.96 (Pa), which was higher than the other hydrogels. The SEM images confirmed that 10% NG–hydrogel composite, can have better mechanical properties. NG-based hydrogel were thermally more stable than hydrogel and nanogel. The presence of different percentage of NG in composite significantly changed Cur release rate in intestinal condition. The Cur release in the intestine was well described by the Peppas model and no release was observed in stomach medium.

Conclusions: The results highlight the advantage of using composite hydrogel as a promising strategy for improving thermal stability and the successful delivery of bioactive materials.

Keywords: Composite, Release, Nanogel-based hydrogel

---

*Correspondence: s.najitabasi@rifst.ac.ir

[1] Department of Food Nanotechnology, Research Institute of Food Science and Technology (RIFST), PO Box 91895-157.356, Mashhad, Iran
Full list of author information is available at the end of the article

Shahbazizadeh *et al. Chem. Biol. Technol. Agric.*   (2022) 9:41

Page 2 of 12

Graphical Abstract
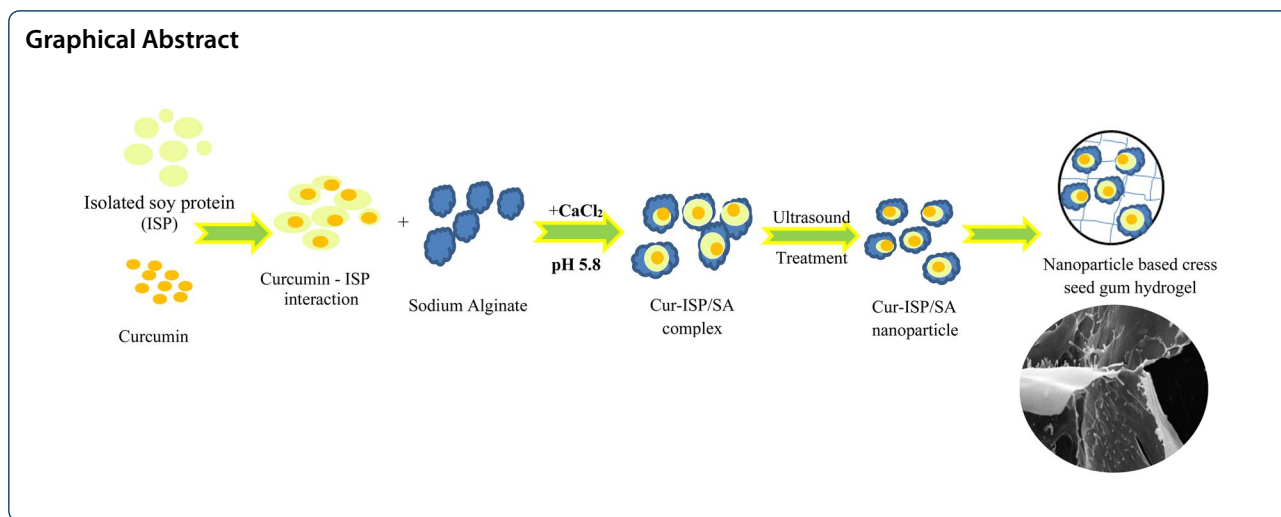
Introduction

Hydrogels are polymeric networks with three-dimensional cross-links which can absorb large amounts of water when immersed in aqueous solution. Hydrogels are solid in terms of shape, and liquid in terms of the high amount of water and the ability of molecules diffusion outside and inside of gel. According to the ability to adjust the hydrogel properties in a wide range of parameters and the fact that various polymer compounds are available, these soft materials are suitable for various applications such as superabsorbent polymers, tissue engineering, and bioactive compound delivery systems [42].

Hydrogels also can load a large fraction of drugs due to their high internal free volume, highly hydrated microstructures of hydrogels lead to slow rates of response to environmental changes, rapid release of hydrophilic drugs, and poor absorption of hydrophobic drugs, which cause limitation in the types and rates of drug release in hydrogel-based systems [43]. Many efforts have been made to improve the mechanical properties of hydrogel networks. One way to achieve fast-response hydrogels is to make hydrogels with thinner and smaller pores such as microgels or nanogels [10]. The high volume/surface ratio in the microgel particles will cause a faster reaction and release [19]. During the release applications of nanogels, the short diffusion path of a nanogel particle generally provides an undesirable release and is much faster than a macroscopic hydrogel [57].

As mentioned above, because of their unique structures and properties, the macro-hydrogels and NPs have shown a very high potential for medical therapeutic and diagnostic applications. However, some inherent limitations of hydrogels and NGs inhibit their widespread applications. In order to overcome these limitations, the development of new systems is needed to integrate the useful properties of nanogels and hydrogels [10, 22]. One approach to solve this challenge is to trap nano or/microgels within hydrogels [10]. The main challenge associated with the small dimensions of microgels can be solved through the development of immobilized microgel matrices, in which individual microgel particles are entrapped inside a hydrogel or cross-linked to form a macroscopic network. Immobilized microgel matrices can provide unique properties and various applications relative to bulk hydrogels or individual microgels [10]. Recent solution, in particular, allows the formation of composite gels that are mechanically stronger due to the integration of support mechanisms, as well as exhibit self-healing properties [8]. Different studies were conducted to develop this structure [2, 34, 44, 58].

The aims of this study were to formulate and characterize curcumin-loaded composites by physical cross-linking method with cress seed (*Lepidium sativum* L.) gum (CSG) hydrogel and isolated soy protein/sodium alginate nanogel. In terms of texture, CSG hydrogel has high elastic and cohesive properties, which is resistant to heating, freezing and maintain their integrity at low temperature [15, 27–29]. These properties are very useful and facilitate the formulation of CSG as a gelling agent in foods that are exposed to high temperatures such as baking, pasteurization and sterilization [42].

Therefore, the objective of this study was to develop soy protein/sodium alginate nanogel-based cress seed gum hydrogel for oral delivery of curcumin. In this study, the influence nanogel-to-hydrogel ratios on hydrogel composite properties (viscoelastic properties, swelling features, differential scanning calorimetry

Shahbazizadeh *et al. Chem. Biol. Technol. Agric.* (2022) 9:41

Page 3 of 12

(DSC), scanning electron microscope (SEM), in vitro release and antioxidant properties) were investigated.

Materials and methods
Materials
Curcumin ($C_{21}H_{20}O_6$, 95% purity), $CaCl_2$, 2,2-diphenyl-1-picrylhydrazyl, dialysis bags and bile salts were purchased from Sigma-Aldrich (USA). CSG powder was prepared from Reyhan Gostar-e-Parsiyan Company. ISP was purchased from Shandong Yuxin Bio-Tech Co. (China). Pepsin and hydrochloride acid were provided from Merck (Germany). Sodium alginate and pancreatin were prepared from Beckmann.Kenko GmbH (Germany) and Wako (Japan), respectively. All the chemicals were of analytical grade.

Preparation of NG-based hydrogel composites
The NG–hydrogel preparation process consists of three steps:

Step I. Cur-ISP/SA nanogels were prepared by Shahbazizadeh et al. [42] method. ISP/SA nanogel was prepared with ISP, SA, and $CaCl_2$ at 1.6% (w/v), 0.069% (w/v), and 0.008% (w/v) concentration, respectively. The ISP dispersion was heated at 95 °C for 30 min and immediately cooled. It was then centrifuged for 15 min at 4000 rpm to remove residual insoluble particles. Ethanol-soluble curcumin 0.04% (w/v) was added dropwise to heated ISP solution. Then, SA was added and the pH of ISP/SA dispersion was adjusted to 5.8 for creation of soluble complex. Cur-ISP/SA dispersion was heated and $CaCl_2$ solution was then added dropwise to the Cur-ISP/SA complex solution on stirrer at a constant rate. The suspensions were sonicated at a pulse mode for 60 s for creation nanogels.

Step II. Physically cross-linked CSG hydrogel was prepared based on Shahbazizadeh et al. [42]. Briefly, 1.5% (w/v) of CSG solution and 0.2% (w/v) of calcium chloride was used for preparation of CSG hydrogel [42]. Part of $CaCl_2$ solution was stored for step III.

Step III. The composites were prepared by dropwise addition of Cur-ISP/SA nanogel suspension into CSG hydrogel and then $CaCl_2$ was added. Different ratios of NGs to hydrogel 10:90, 15:85 and 20:80 (v/v) were prepared and named 10% NG–hydrogel, 15% NG–hydrogel, and 20% NG–hydrogel, respectively.

Scanning electron microscopy (SEM) studies
A LEO 1450vp SEM (20 kV, Germany) was used to clarify the morphology of the freeze-dried NG-based hydrogels. Before the analysis, the samples were coated with gold under a vacuum.

Frequency sweep test
The viscoelastic test of NG-based hydrogels was conducted by Physica MCR302 controlled strain rheometer (Anton Paar GmbH, Germany) that was equipped with the cone plate system (4 angle, 0.206 mm gap, and 25 mm diameter). A strain sweep test (1–100%) was first performed to identify the linear viscoelastic range of each hydrogel composite. The frequency sweep test was conducted at a frequency range of 0.01–10 Hz at a constant strain of 0.5% (LVE region). All rheological measurements were conducted at 20 °C [56]. MATLAB 2021 and Physica Rheometer Data Analysis software (Rheoplus/32, version V3.40) were used to analyze storage modules (G'), loss modules (G"), Complex viscosity (η^*), and loss tangent (tanδ) in linear viscoelastic region.

Differential scanning calorimetric (DSC) measurements
The thermal properties of CSG composites were measured by DSC (IRSA DSC100, Iran). The samples were heated from 10 to 250 °C at a rate of 10 °C/min [31]. According to DSC results, melting (T_P), and onset (T_O) temperatures and enthalpy values (ΔH) were reported.

Swelling degree
In order to evaluate the swelling degree of hydrogels, the lyophilized pre-weighted samples were immersed in 100 ml of phosphate buffer solution with pH 6.8 (25 °C). The swollen composites were weighted for 24 h. Based on the results, the swelling degree (SD) was calculated by the following equation [18, 47]:

$$SD = \frac{W_s - W_d}{W_d} * 100, \tag{1}$$

where W_d and W_s are the weights of the dried sample and swollen sample, respectively. The swelling degree of gels reaches equilibrium described by SD. The samples were prepared in triplicates.

In vitro curcumin release studied
In vitro release of curcumin from formulations was determined at 37 °C in gastrointestinal medium. Gastric phase fluid included 100 mL of simulated gastric fluid (containing double distilled water, 0.3 (gr) pepsin and 0.2 (gr) NaCl) adjusted to pH 1.2. Intestinal phase fluid was prepared by 100 ml of simulated intestinal fluid (containing double distilled water, 0.1 (gr) pancreatin, and 0.85 (gr) NaCl and 0.3 (gr) bile salt in phosphate buffer solution (pH 6.8, 5 mM) adjusted to pH 6.8 with NaOH 0.1 M [14]. HCl and NaOH 0.1 N were used to mimic the main pH conditions of the stomach and small intestine, respectively.

Shahbazizadeh *et al. Chem. Biol. Technol. Agric.* (2022) 9:41

Page 4 of 12

Curcumin release from NG-based hydrogels was studied using a dialysis method. Dialysis bags (12–14 kDa), Sigma Aldrich were soaked in distilled water at room temperature for 12 h to remove the preservative materials, followed by rinsing thoroughly in distilled water. Cur-hydrogel was transferred to the dialysis bag. The dialysis bag was closed at both ends and then immersed in the gastrointestinal release medium on the shaker (100 rpm) at a constant temperature (37 °C).

The release medium was withdrawn (2 ml) for analysis at different time intervals (0, 30, 60, 90, 120, 150, 180 and 240 min). Then, replaced with fresh medium (2 ml). The released curcumin was evaluated spectrophotometrically (420 nm). The test was done in triplicate.

Assessment of release kinetics

The release kinetic was studied based on zero-order, first-order, Higuchi, and Peppas models [26]:

$$M_0 - M_t = k_0 \cdot t, \tag{2}$$

where M_0, M_t, t, and k_0 are the initial concentrations of curcumin in nanogels and the concentration of curcumin in nanogels at time t, respectively. k_0 is the zero-order release constant:

$$Ln(M_0/M_t) = k \cdot t. \tag{3}$$

k is the first-order release constant:

$$Q = k_H t^{1/2}, \tag{4}$$

where k_H is the Higuchi dissolution constant:

$$M_t/M_\infty = k_P t^n, \tag{5}$$

where M_t/M_∞, n, and k_p are the fraction of curcumin released at time t, diffusion exponent indicative, and kinetic constant, respectively.

Antioxidant stability of entrapped curcumin against heating

Curcumin-loaded nanoparticles–hydrogel composites were heated for 15 min at 180 °C. DPPH (2,2-diphenyl-1-picrylhydrazyl) radical scavenging activity was measured using the method of Tapal and Tiku [49]. Preheated samples were firstly sonicated and 1 ml of each sample was added to 1 ml DPPH (0.2 mM), and then vigorously mixed. After incubation for 30 min, the resulting solution was centrifuged at 8000 rpm for 10 min and the absorbance was measured at 517 nm using a UV-spectropho-tometer. The solution without any sample was considered as the control. The antioxidant activity (%) was calculated according to Eq. 6:

$$\text{Antioxidant activity (\%)} = \frac{A\,control - A\,sample}{A\,control} * 100, \tag{6}$$

where A blank is the absorbance of the DPPH solution without the sample; and A sample is the absorbance of the test solution [50].

Statistical analysis

Results were expressed by means ± standard deviation. A completely randomized design was used for statistical analysis. The data were analyzed by analysis of variance (ANOVA) and Duncan multiple range test (P ≤ 0.05).

Results and discussion

SEM studies

The microstructures of NG-based hydrogel are presented in Fig. 1. All hydrogels exhibited the typical porous cross-linked structure. Curcumin-loaded ISP/SA NGs are clearly observed in composites SEM images. Also, for all composites, typical wrinkled structure of CSG was easily found in more amplification of SEM images. NG–hydrogel composite structures are changed by varying NG:hydrocolloid ratios. The structure of 10% NG composite was more cross-linked and porous. It might be attributed to the potentiation of nanoparticle, which increased and enhanced cross-linking sites. Moreover, no obvious two-phase structure was observed in these images, revealing that NGs were dispersed on the CSG sheets on a large scale [55]. By increasing the NG participation to above 15% (v/v), pore size of hydrogel became bigger. Since composites with denser and more regular structure can be stronger, it can be concluded that composites with lower NG content have better mechanical properties. These results confirmed the results of frequency sweeping test (Table 1). Pore size of 20% NG composite was greater than other samples, indicating that the addition of NG did not destroy the structure of the hydrogel network. Pilevaran et al. [34] produced whey protein–xanthan gum hydrogel by incorporation of basil seed gum nanoparticles (BSG NPs). They reported by adding BSG NPs to the hydrogel matrix, the number of holes increased, but the size of holes reduced. Increasing the percent of BSG NPs (from 1 to 3%) resulted in bigger holes through the fibril connections in the matrix [34].

Dynamic rheological properties

The viscoelastic properties of NG-based hydrogels, including storage and loss modules and loss tangent (at f = 1 Hz, τ = 0.1 Pa and 20 °C) are summarized in Table 1. Three types of system can be recognized by frequency

Shahbazizadeh *et al. Chem. Biol. Technol. Agric.*   (2022) 9:41

Page 5 of 12
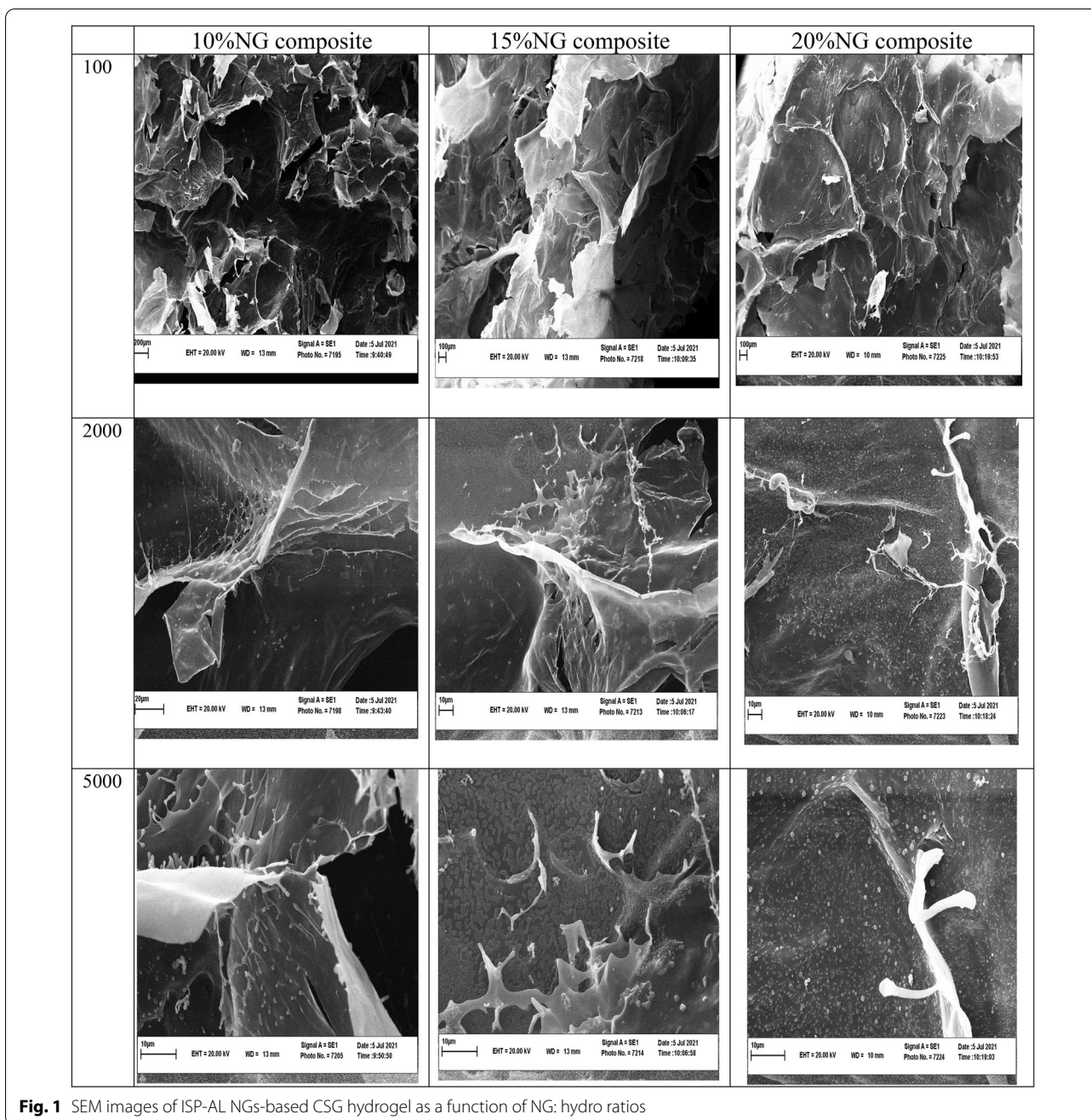
Fig. 1 SEM images of ISP-AL NGs-based CSG hydrogel as a function of NG: hydro ratios

Table 1 Dynamic rheological parameters of ISP/SA nanogel-based CSG hydrogel composites and CSG hydrogel determined by frequency sweep test at $f = 1$ Hz, constant strain of 0.5% and 20 °C

Sample	G′ (Pa)	G″ (Pa)	tanδ	Pa.s))*η	Slope of η*.f
10% NG composite	60.96	8.91	0.146	65.66	− 1.029
15% NG composite	20.45	3.86	0.189	17.84	− 1.026
20% NG composite	11.87	2.69	0.227	17.15	− 0.864
CSG hydrogel	37.69	8.13	0.216	38.55	− 1.116

sweep measurements: dilute solutions, concentrated solutions and gels. For gels, G′ is always greater than G″ in applied frequency range. In dilute polysaccharide solutions, G″ modulus is greater than G′ that close to each other at higher frequencies. For concentrated systems, G′ value is smaller than G″ at low frequency and cross-over each other in middle of the frequency range. In all hydrogel samples, the G′ was higher than the G″ (data not shown), which shows gel-type viscoelastic behavior. A higher storage modulus than a loss modulus indicates the high ability of molecular chains to form a network.

Shahbazizadeh *et al. Chem. Biol. Technol. Agric.*   (2022) 9:41

Page 6 of 12

Existence of more molecular interactions in NG–hydrogel leads to enhancement of viscoelastic behavior. Clark and Ross-Murphy [7] have chosen structural liquid term for these fluids which represents an intertwined network in these solutions structures even at high frequencies. The storage modulus of CSG hydrogel and 10, 15 and 20% NG-based hydrogel was 37.69, 60.96, 20.45 and 11.87 (Pa), respectively. The loss modulus (G') of CSG hydrogel and 10, 15 and 20% NG composite was 8.13, 8.91, 3.86 and 2.69 (Pa), respectively. The NG:hydrogel ratios played a pivotal role in the development of elastic properties. Cheng et al. [5] also reported mechanical properties of the composites can be controlled by changing the NG:hydrogel ratio [5]. The highest amount of storage and loss modulus was related to the 10% NG–hydrogel, which indicated that the 10% NG composite had stronger elastic properties than the CSG hydrogel and other NG–hydrogel composites. 10% NG–hydrogel had a more regular structure (Fig. 1), which may lead to a better mechanical property. Cooperation of higher ratios of NGs (15 and 20% NG) in hydrogel decreased the storage and loss modulus of composites. These discrepancies may be explained by the uniform distribution of ISP/SA nanogel in the 10NG–hydrogel structure. ISP/SA NGs can help to strengthen the physical connection points, which is mainly due to the molecular interaction between the CSG hydrogel sheet structure and SA chains in NGs [55]. The SA chains of NGs can join with the CSG chains by ionic and hydrogen interactions, which results in the formation of a double network structure, resulting in more elastic gel composite in 10NG-hydrogel.

Diminishing of cross-links was an important property leading to decrease of storage and loss modulus at 15% and 20% NG composites [8, 53]. Higher amounts of nanogels and less CSG hydrogels reduced the structural integrity and showed lower G' values. Pilevaran et al. [34] reported the incorporation of basil seed gum nanoparticles (BSG NPs) in whey protein concentrate–xanthan (WPC–XG) hydrogel decreased gel strength noticeably, which was related to the open microstructure of the WPC–XG–(BSG NPs) hydrogel composite [26].

The loss tangent is the ratio of the loss modulus to the storage modulus [30]. Another way of quantifying the gel strength and gelation is to look at the phase angle, δ, given by the relation tan δ=G''/G'. The lower value of δ, the more elastic the material [13], where the loss tangent value is less than 1, indicates the elastic (solid-like) behavior is prominent, while the loss tangent greater than 1 corresponds the liquid-like gel behavior. The values of loss tangent above 0.1 mean that the samples are not real gels and have a structure between concentrated biopolymer and real gel [26]. Loss tangent values obtained from the hydrogels were between 0.15 and 0.23 (Table 1),

which indicate their ability to form a weak gel. The composite systems had a structure between a concentrated biopolymer and a real gel. The lowest amount of loss tangent was observed in the 10% NG–hydrogel (0.15), which was associated with the formation of a stronger interwoven network, indicating its high elastic behavior. The values of loss tangent increased with increasing the concentration of NG. Other researchers have reported solid behavior of CSG gel. These gums produce "weak-gel" networks through weak communications between hard and orderly molecular structures in solution [38]. Studies on the loss tangent of polymer systems offer high numerical ranges (0.2–0.3) for amorphous polymers and low numerical ranges (close to 0.01) for crystalline polymers and gels.

The complex viscosity values (η^*) of hydrogels decreased with increasing frequency (Fig. 2). The complex viscosity of the 10% NG–hydrogel (65.66 Pa.s) was higher than the 15, 20% NG–hydrogel and CSG hydrogel (17.84 and 17.15, 38.55 Pa.s, respectively) (Table 1). The cross-linking between NG and CSG hydrogel created a more uniform and packed structure in 10NG–hydrogel, which improved η^* (Carbinatto, de Castro, Evangelista, & Cury, 2014).

The slope of η^*-*f* is the other parameter, indicates the resistance of the gel. The slope of η^*-*f* of hydrogels were 0.864 to -1.116 (Table 1). Higher value of the slope in this study confirms the presence of more elastic gels. The slope of η^*-*f* of 10%, 15% NG–hydrogel and CSG hydrogel were the same. In contrast, 20% NG–hydrogel showed a small slope of η^*-*f*, which was (-0.86). The 20%NG–hydrogel provides a weak gel. The (η^*-*f*) close to (-0.8)
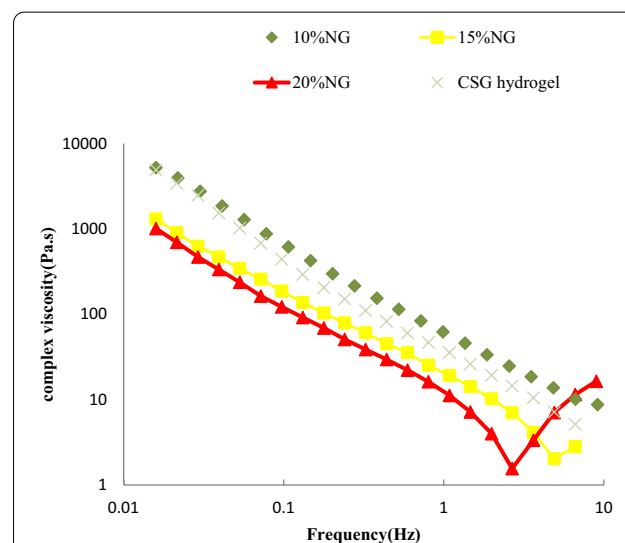
Fig. 2 Complex viscosity changes of 10%, 15%, 20% NG–hydrogel composites, and CSG hydrogel vs. frequency

Table 2 Thermal properties of CSG hydrogel, ISP/SA nanogel, curcumin, ISP/SA nanogel–CSG hydrogel, and Cur-ISP/SA nanogel–CSG hydrogel

H (J/g) Δ	T_m (ºC)	T_o(ºC)	Sample
10% NG composite free Cur			
57.86	90.2	72.9	1st peak
39.81	338.0	318.3	2nd peak
15% NG composite free Cur			
44.03	89.7	64.0	1st peak
37.01	336.5	318.6	2nd peak
20% NG–hydrogel free Cur			
38.75	87.4	68.8	1st peak
38.10	332.2	311.7	2nd peak
Cur-10% NG–hydrogel			
23.05	90.1	57.7	1st peak
36.7	337.8	331.7	2nd peak
			Cur-15%NG–hydrogel
49.86	87.9	67.3	1th peak
53.08	336.1	317.0	2thpeak
Cur-20% NG–hydrogel			
54.87	93.2	62.4	1st peak
49.52	336.1	315.7	2nd peak
CSG hydrogel			
26.65	90.0	76.4	1st peak
7.65	337.4	325.7	2nd peak
ISP/SA nanogel			
23.05	312.2	275.6	Peak
Cur-ISP/SA nanogel			
46.66	69.8	54.2	1st peak
44.97	331.4	274.7	2nd peak
44.36	208.5	178.0	Curcumin

indicated a weak polysaccharide gel obtained by entanglement and interference of random chains of polysaccharides [23]. Therefore, it can be concluded that the NG plays a major role in the elastic behavior of the hydrogel.

DSC studies

Table 2 shows the DSC thermogram of curcumin, CSG hydrogel and curcumin-free/curcumin-loaded NG–hydrogel composites. An endothermic peak at 208.05 °C was observed, which indicates the melting temperature of the pure curcumin. The onset temperature (T_o) and melting enthalpy (ΔH) of curcumin were 178.0 °C and 44.36 (J/g), respectively.

ISP/SA nanogel shows endothermic and exothermic peaks. The onset temperature, melting temperature and melting enthalpy (ΔH) of exothermic peak were 274.7 °C, 331.4 °C, and 9744(J/g), respectively. In thermographs of composites, all samples showed endothermic peaks below 100 ∘C, attributed to water evaporation (87.40, 89.70 and 90.20 °C for 20, 15 and 10% NG composites, respectively)

[38]. ΔH of 20, 15 and 10% NG composites were 38.75, 44.03 and 57.86 (J/g), respectively (Table 2). When curcumin was loaded in the composite network, endothermic peak had no noticeable change. Cooperation of NGs increased ΔH of NG–hydrogel when compared with CSG hydrogel.

The 20, 15 and 10% NG–hydrogels showed an exothermic peak at 332.2, 336.5 and 338.3 °C due to sample destruction. ΔH of exothermic peak of 20, 15 and 10% NG–hydrogels were and were 38.75, 44.03 and 57.86(J/g)), respectively. After curcumin loading, degradation temperature of the 20, 15 and 10% NG composites were shifted to 336.1, 336.1 and 337.8 °C and ΔH were 49.52, 53.08 and 36.7 (J/g), respectively.

Severe endothermic peak specific for curcumin was not observed in any of the composite formulations, which confirms the molecular dispersion of curcumin in the polymer matrix [25]. Displacement of exothermic peak and ΔH values in the curcumin-loaded composites indicated a successful interaction of the hydrogel and the curcumin-loaded nanogel [24]. The presence of similar peaks with minor changes confirmed the interaction between the active sites of the hydrogel and/curcumin-loaded nanogels and molecular dispersion of curcumin-loaded nanogels in the composite [39].

Other researchers have made similar observations in their studies on drug release [20, 25]. Rao, Mallikarjuna and coworkers synthesized poly 2-Hydroxyethylmethacrylate-co-Acrylamidoglycolic acid-based (HEMA-co-AGA) hydrogels for the controlled release of 5-fluorosyl. DSC was performed to understand the crystalline nature of the hydrogel and the drug after coating in the hydrogel. DSC results showed that 5-fluorosyl showed a sharp peak at 285 °C due to polymorphism and melting, but in the case of HEMA-co-AGA hydrogels loaded with 5-fluorosil, no characteristic peaks were observed at this temperature which indicate 5-fluorosyl is molecularly dispersed in the hydrogel network [36].

The endothermic peak temperature as well as the degradation temperature in all free curcumin hydrogels increased by reducing NG to hydrogel reducing, which shows thermal resistance of the composites increased by increasing the hydrogel concentration. It has been shown that this NG–hydrogel structure leads to slow conduction of heat [12]. Its structure disintegrates only at high temperatures, and these data show that the 10% NG composite was thermally more stable than the other samples. Increasing the degradation temperature of free curcumin formulations increased as the concentration of the cross-linker agent increased, which was consistent with the results reported by other researchers [12]. However, Cur-NG–hydrogel did not follow this trend.

Shahbazizadeh *et al. Chem. Biol. Technol. Agric.*   (2022) 9:41

Page 8 of 12

Table 3 Swelling degree of ISP/SA nanogel, ISP/SA nanogel-based CSG hydrogel composites, and CSG hydrogel

System	Swelling degree
CSG hydrogel	105.96±12.99[b]
10% NG-hydrogel composite	206.20±21.38[a]
15% NG-hydrogel composite	165.88±8.73[ab]
20% NG-hydrogel composite	126.26±26.94[b]
ISP/SA nanogel	65.28±0.38[c]

Different small letter superscripts in a column indicate significant differences at $p < 0.05$

Swelling degree

The swelling degree of composites was measured as an indicator of water absorption capacity. Diffusion of the medium into the polymeric network and subsequently to the core of the hydrogels, followed by the polymer chains relaxation, causes the swelling process [34]. 10, 15 and 20 NG–hydrogels had 206.20, 165.88 and 126.26% swelling degrees, respectively (Table 3). All NG–hydrogels had more swelling value than CSG hydrogel (105.96) ($p < 0.05$). Increasing the amount of NG lead to formation of NG aggregates and is associated with large pore size. These pores can cause more water transferring to the hydrogel network, leading to higher swelling [6].

Composites containing 10% NG had the highest swelling degree ($p < 0.05$). 15% and 20% NG–hydrogel had no significant difference in terms of swelling degree ($p < 0.05$). The presence of CSG hydrogel increases the number of hydrophilic groups, which results in more hydration and swelling [51]. The presence of NG: HYD ratio of 10:90, expands the composite network and increases the porous matrix, and consequently the composite absorbs more water [9]. Elhadi et al. investigated the swelling properties of chitosan hydrogel based on curcumin–silver nanocomposite. They found that the swelling degrees of curcumin–silver/chitosan hydrogel were higher than chitosan hydrogel at pH 4 and 7. This may be due to the presence of curcumin–silver nanoparticles in the hydrogel, which expands the formed hydrogel network [9]. But higher amounts of NGs and lower amount of hydrogel (15:85 and 20:80) reduced the swelling degree. May be, the ratio of NGs to CSG hydrogel was not appropriate to improve the swelling properties. In higher ratios of NGs to hydrogel, the number of carboxyl groups reduced because of the linking of high number of NGs and –COOH group of CSG polymers. Therefore, the electrostatic repulsion between –COO- groups becomes weak, and decreases the swelling ratio (%) of the hydrogel [34]. In addition, Tansaz and colleagues (2018) prepared hydrogel based on soy protein isolate by adding different ratios of ISP and SA and investigated their

physicochemical properties. In this study, they found that water uptake decreased with increasing soy protein isolate concentration, which related to the higher hydrophilicity of SA compared to ISP [48].

In vitro release

The release profile of curcumin from composite hydrogel formulations under simulated gastrointestinal conditions is presented in Fig. 3. In stomach environment no release of curcumin was observed after 120 min in all samples, which indicates the integrity of the system was maintained in the stomach condition. The results showed that the curcumin trapped by the hydrogel composite is well protected against the pepsin. The release rate of the bioactive compound from the composite matrix depends on the interaction between the bioactive compound and the polymer molecule, the solubility of the bioactive compound and the swelling of the hydrogel in the aqueous medium. CSG hydrogel can swell or shrink depending on the pH and ionic strength dispersed in the environment [15, 45]. At low pH, the carboxyl groups in the structure of the hydrogel polysaccharide chain are protonated. In the absence of repulsive forces, hydrogen bonds are formed between CSG chains, and shrinkage occurred under acidic conditions [6]. Since the CSG chains are anionic polysaccharide, the CSG hydrogel-based composite shrunk in an acidic medium, reduced pore size and, consequently, curcumin release did not occur in
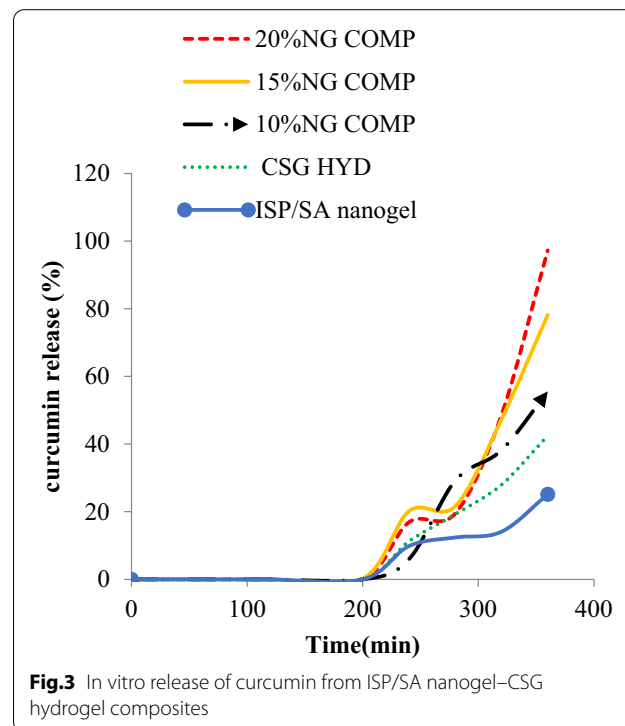
Fig.3 In vitro release of curcumin from ISP/SA nanogel–CSG hydrogel composites

Shahbazizadeh *et al. Chem. Biol. Technol. Agric.*   (2022) 9:41

Page 9 of 12

the gastric environment. Also, due to the formation of hydrogen bonds, CSG is converted to an insoluble acidic compound, which controls the diffusion of water and prevents the decomposition of the matrix. Presence of cross-linker agent reduced the solubility of the polymer matrix in acidic conditions, which can be an effective approach to the sustainable release of nutraceuticals and drugs [46]. This result was consistent with the reports of other researchers [6, 21, 26]. The release of curcumin in intestinal condition was faster than acidic condition. This is due to the fact that the CSG is anionic gum [37] and polymer networks swell in intestinal environment.

The different ratios of NG:HYD in composite formulation changed significantly Cur release rate in intestinal condition. As shown in Fig. 3, the release rates of curcumin from ISP-AG nanogel and CSG hydrogel were 25.15 and 42.50, respectively. Contrary to our expectations, the release of curcumin increased with the incorporation of nanogels in the structure of the hydrogel (NG–hydrogel composite) in comparison with nanogel and CSG. The release of curcumin depends on the composition of the polymer matrix [51]. These results were also consistent with observations of swelling degrees in composites (Table. 3). The swelling rate of the composites affected the release kinetics of curcumin [51]. High swelling degrees indicated the imminent collapse of the system [11]. The participation of NGs in CSG hydrogel structure increased water absorption, swelling and subsequent degradability properties in phosphate buffer pH 6.8 compared to CSG hydrogel or NGs. The high swelling ratio of the composite creates wider surface spaces for curcumin release [3].

Curcumin release profiles from formulations containing different nanogel ratios are shown in Fig. 3. The maximum Cur release was observed in 15 and 20% NG composites (97.29% and 78.16%, respectively) ($p < 0.05$). The Cur release from 10NG–hydrogel was 55.66%. The first step towards elucidating the release mechanism is to understand whether the difference in release profile of these formulations is due to a change in the structure of the hydrogel network or as a result of a structural change in the nanogel [17]. The reason for this may be attributed to the increase in viscoelastic properties of 10NG–hydrogel, which in turn increased the erosion and release

resistance [40]. The Cur release from the composites was strongly affected by their viscosity. Increment of hydrogel content in the composite structure means increment of hydrogel layer around the nanogel. NG:HYD volumetric ratio in 10NG:90HYD increased the complex viscosity and created a harder matrix gel structure [35]. In other words, reinforcement of intermolecular forces between CSG hydrogel and ISP/SA nanogels results in a dense composite structure of 10NG composite that can delay the release of curcumin [33]. These results were consistent with SEM studies, dynamic rheology and complex viscosity (Figs. 1 and 2 and, Table 1).

The delay in the release of curcumin in the 10% NG composite, despite the higher swelling, was due to the entrapment of curcumin molecules in swollen granules with high tortuosity. The diffusion phenomenon depends on the concentration of CSG and calcium chloride salt as cross-linkers [17].

In a similar study, a gel structure was used to load the Liz-Pro-Wall (KPV) in NGs for drug delivery in the gastrointestinal tract. Nanoparticles loaded with KPV peptides were coated in hydrogel to form a nanoparticle–gel formulation that was stable in gastric juice at pH 2 for 24 h. However, when exposed to intestinal juice at pH values above 5, the hydrogel structure rapidly decomposed and the nanoparticles were transported to the large intestine [11].

Kinetics of curcumin release

The release data were fitted with the zero-degree, first-degree, Higuchi and Korsmeyer–Peppas models, and the resulting parameters are summarized in Table 4. The release rate of curcumin in the small intestine from all composite formulations follows the Peppas kinetic model. The correlation coefficient of Peppas model for 10, 15 and 20% NG–hydrogels were 0.99, 0.97 and 0.98, respectively.

The n value of Korsmeyer–Peppas model shows the release mechanism. In the case of a cylinder-shaped hydrogel-drug delivery system, the release mechanism follows a quasi-Fickian diffusion if $n < 0.45$, and it follows Fickian diffusion if $n = 0.45$. This indicated the drug is smaller than the mesh size and can quickly diffuse

Table 4 Curcumin release kinetic from ISP/SA nanogel-based CSG hydrogel composites

NG incorporation (%)	Zero order		First order		Higuchi		Peppas		
	K_0%min	R^2	K_1 %min	R^2	K_H %min$^{1/2}$	R^2	K_p %min^n	n	R^2
10	0.25	0.91	0.62	0.91	3.28	0.88	0.84	0.77	0.94
15	0.33	0.96	1.57	0.96	4.27	0.78	0.60	0.88	0.97
20	0.32	0.97	0.89	0.97	4.83	0.78	0.17	0.96	0.98

Shahbazizadeh *et al. Chem. Biol. Technol. Agric.*   (2022) 9:41

Page 10 of 12

through the hydrogel mesh. On the other hand, if the drug size is similar to the hydrogel mesh size, its diffusion is slower. If $n > 0.89$, the release mechanism follows Case II transport and the release happens because of the swelling of the system. If $0.45 < n < 0.89$, the release mechanism follows anomalous transport, which is a combination of diffusion and swelling [52].

The power of (n) in Peppas model for 10, 15 and 20% NG composites were 0.77, 0.88 and 0.96, respectively. The 10 and 15NG–hydrogel composites followed anomalous transport, which is a combination of diffusion and swelling. In the case of release by swelling, drug size is larger than mesh size; hence the drug is entrapped in the hydrogel and can only be released by deformation or degradation of the latter. The release mechanism of 20% NG composite followed Case II transport and the release happens because of the swelling of the system. In the 20% NG composite, the continuous release of about 97.26% was observed. Hence, the release of curcumin encapsulated in the particles and in the hydrogel suggests that during the first phase, physically entrapped nanoparticles are quickly released upon polymer swelling, resulting in a fast release of curcumin in the first phase, followed by a second phase of release of the particles that are chemically bound to the hydrogel [41].

This difference can be due to a decrease in the concentration of Ca^{2+} ions. It seems that with decreasing $CaCl_2$ concentration, the formation of structured barrier matrix is reduced, which can enhance the penetration of water into the matrix and outflow of curcumin into the aqueous medium. This may explain the change of the release mechanism in 20NG–hydrogel when the Ca^{+2} concentrations decreased [1].

Evaluation of DPPH scavenging activity

The antioxidant activity of curcumin plays a major role in its therapeutic effect. The results of the antioxidant activity are summarized in Table 5. All samples had antioxidant properties. But, there was a significant difference between the three formulations in terms of DPPH scavenging activity. The lowest antioxidant activity was observed in the 10% NGs–hydrogel composite (37.18%), which was statistically different from the other two composites ($p < 0.05$). With increasing the amount of NG containing curcumin from 10 to 20% in the formulation, the amount of DPPH free radical scavenging activity increased to 69.58%. These results were consistent with the observations of other researchers [50].

The results showed heat treatment had no significant effect on the antioxidant activity of 10 and 15% NG composites ($p < 0.05$). By reducing the contribution of hydrogel from 90 to 80%, the antioxidant activity was significantly reduced after heating. This effect is probably due to the higher protective effect of the hydrogel polymer matrix. CSG hydrogel layer surrounded the curcumin-loaded nanogels and protected curcumin [32]. Xiong et al. [54] investigated the antioxidant properties of nanocomposite hydrogel based on polydopamine containing poly (N-isopropyl acrylamide) nanoparticles. They reported nanocomposite gels had high antioxidant properties. The inhibitory activity of nanocomposite hydrogels increased markedly with increasing polydopamine content [54].

Conclusion

In this study, a hydrogel composite system consisting of different ratios of ISP/SA nanogel in CSG hydrogel was investigated. The mechanical properties of the composite could be controlled by varying the CSG hydrogel:ISP/SA nanogel ratio. According to the result 10% NG–hydrogel shows the highest G'. Similar results were observed in the loss modulus. At first, the loss modulus of 10% NG composite (8.91 Pa) was increased compared to the hydrogel (8.13 Pa). However, the loss modulus of 15 and 20% NG composites decreased to 3.86 and 2.69 Pa, respectively, compared to hydrogel. The lowest amount of tan δ was observed in the 10% NG composite (0.14), which was associated with the formation of a stronger cross-linked network. This parameter has effects on swelling and rheological behavior of composites while maintaining their sustained release. The dynamic mechanical properties of composites and SEM images showed more homogeneous and stable cross-linked inner structure of 10% NG composite. Finally, the results of in vitro drug release profile indicated that the composite could control drug release or bind drug inside depending on the NG ratio of formula. 10% NG composite can be a promising solution that can release active compounds with a suitable kinetics, and this study provided a simple approach to design and fabricate functional system for curcumin delivery.

Table 5 Effect of heat treatment on antioxidant activity of Cur-ISP/SA nanogel-based CSG hydrogel composites

Sample	DPPH scavenging activity (%) before heating	DPPH scavenging activity (%) after heating
Cur-10% NG hydrogel	37.18 ± 5.63[cA]	35.78 ± 1.38[cA]
Cur-15% NG hydrogel	43.08 ± 0.63[bA]	41.58 ± 1.69[bA]
Cur-20% NG hydrogel	69.58 ± 1.03[aA]	57.98 ± 0.50[aB]

Different small letter superscripts in a column indicate significant differences at $p < 0.05$

Different capital letter superscripts in a row indicate significant differences at $p < 0.05$

Shahbazizadeh *et al. Chem. Biol. Technol. Agric.*   (2022) 9:41

Page 11 of 12

Declarations

Ethics approval and consent to participate
This study does not involve any human or animal testing.

Consent for publication
Not applicable.

Competing interests
The authors declare that they do not have any conflict of interest.

Author details
[1]Department of Food Nanotechnology, Research Institute of Food Science and Technology (RIFST), PO Box 91895-157.356, Mashhad, Iran. [2]Department of Food Chemistry, Research Institute of Food Science and Technology (RIFST), PO Box 91895-157.356, Mashhad, Iran.

References
1. Al-Remawi M. Quality by design of curcumin-loaded calcium alginate emulsion beads as an oral controlled release delivery system. J Excip Food Chem. 2016;6(2):930.
2. Bae JW, Go DH, Park KD, Lee SJ. Thermosensitive chitosan as an injectable carrier for local drug delivery. Macromol Res. 2006;14(4):461–5.
3. Bardajee GR, Pourjavadi A, Ghavami S, Soleyman R, Jafarpour F. UV-prepared salep-based nanoporous hydrogel for controlled release of tetracycline hydrochloride in colon. J Photochem Photobiol B. 2011;102(3):232–40.
4. Carbinatto FM, de Castro AD, Evangelista RC, Cury BS. Insights into the swelling process and drug release mechanisms from cross-linked pectin/high amylose starch matrices. Asian J Pharm Sci. 2014;9(1):27–34.
5. Cheng Q, Ding S, Zheng Y, Wu M, Peng Y-Y, Diaz-Dussan D, Cui Z. Dual cross-linked hydrogels with injectable, self-healing, and antibacterial properties based on the chemical and physical cross-linking. Biomacromol. 2021;22(4):1685–94.
6. Cinay GE, Erkoc P, Alipour M, Hashimoto Y, Sasaki Y, Akiyoshi K, Kizilel S. Nanogel-integrated pH-responsive composite hydrogels for controlled drug delivery. ACS Biomater Sci Eng. 2017;3(3):370–80.
7. Clark AH, & Ross-Murphy SB. Structural and mechanical properties of biopolymer gels. In Biopolymers. Berlin: Springer. 1987. p. 57-192.
8. Dannert C, Stokke BT, Dias RS. Nanoparticle-hydrogel composites: from molecular interactions to macroscopic behavior. Polymers. 2019;11(2):275.
9. El-Hady A, Saeed S. Antibacterial properties and pH sensitive swelling of in situ formed silver-curcumin nanocomposite based chitosan hydrogel. Polymers. 2020;12(11):2451.
10. Farjami T, Madadlou A. Fabrication methods of biopolymeric microgels and microgel-based hydrogels. Food Hydrocolloids. 2017;62:262–72.
11. Gao W, Zhang Y, Zhang Q, Zhang L. Nanoparticle-hydrogel: a hybrid biomaterial system for localized drug delivery. Ann Biomed Eng. 2016;44(6):2049–61.
12. Han C, Xiao Y, Liu E, Su Z, Meng X, Liu B. Preparation of Ca-alginate-whey protein isolate microcapsules for protection and delivery of L. bulgaricus and L. paracasei. Int J Biol Macromol. 2020;163:1361–8.
13. Hao X, Liu H, Xie Y, Fang C, Yang H. Thermal-responsive self-healing hydrogel based on hydrophobically modified chitosan and vesicle. Colloid Polym Sci. 2013;291(7):1749–58.
14. Hu Y, Xiao YW, Jin RX, Juan G. Study on the preparation and drug release property of soybean selenoprotein/carboxymethyl chitosan composite hydrogel. J Polym Eng. 2018;38(10):963–70.
15. Jannasari N, Fathi M, Moshtaghian SJ, Abbaspourrad A. Microencapsulation of vitamin D using gelatin and cress seed mucilage: Production, characterization and in vivo study. Int J Biol Macromol. 2019;129:972–9.
16. Jelvehgari M, Mobaraki V, Montazam SH. Preparation and evaluation of mucoadhesive beads/discs of alginate and algino-pectinate of piroxicam for colon-specific drug delivery via oral route. Jundishapur J Nat Pharm Prod. 2014;9(4):e16576.
17. Josef E, Zilberman M, Bianco-Peled H. Composite alginate hydrogels: an innovative approach for the controlled release of hydrophobic drugs. Acta Biomater. 2010;6(12):4642–9.
18. Joung HJ, Choi MJ, Kim JT, Park SH, Park HJ, Shin GH. Development of food-grade curcumin nanoemulsion and its potential application to food beverage system: antioxidant property and in vitro digestion. J Food Sci. 2016;81(3):N745–53.
19. Khoshmanzar M, Ghanbarzadeh B, Hamishekar H, Sowti M, Rezayi Mokarram R. Investigation of effective parameters on particle size, zeta potential and steady rheological properties of colloidal system based on carrageenan-caseinate nanoparticles. Res Innov Food Sci Technol. 2013;1(4):255–72.
20. Kurkuri MD, Kulkarni AR, Kariduraganavar MY, Aminabhavi TM. In vitro release study of verapamil hydrochloride through sodium alginate interpenetrating monolithic membranes. Drug Dev Ind Pharm. 2001;27(10):1107–14.
21. Mehregan Nikoo A, Kadkhodaee R, Ghorani B, Razzaq H, Tucker N. Control of swelling and release rate of electrospray fabricated calcium alginate microparticles by freeze-thaw cycles. Iranian Journal Of Food Science And Technology. 2015;13(1):37–49.
22. Meid J, Friedrich T, Tieke B, Lindner P, Richtering W. Composite hydrogels with temperature sensitive heterogeneities: influence of gel matrix on the volume phase transition of embedded poly-(N-isopropylacrylamide) microgels. Phys Chem Chem Phys. 2011;13(8):3039–47.
23. Morris ER. Shear-thinning of 'random coil' polysaccharides: Characterisation by two parameters from a simple linear plot. Carbohyd Polym. 1990;13(1):85–96.
24. Mundlia J, Ahuja M, Kumar P, Pillay V. Pectin–curcumin composite: synthesis, molecular modeling and cytotoxicity. Polymer Bulletin. 2019;76(6):3153–73.
25. Nagarjuna G, Kumara Babu P, Maruthi Y, Parandhama A, Madhavi C, Subha M. Sodium alginate/tragacanth gum blend hydrogel membranes for controlled release of verapamil hydrochloric acid. Indian J Adv Chem Sci. 2016;4:469–77.
26. Naji-Tabasi S, Razavi SMA, Mehditabar H. Fabrication of basil seed gum nanoparticles as a novel oral delivery system of glutathione. Carbohyd Polym. 2017;157:1703–13.
27. Naji S, Razavi SM. Functional and textural characteristics of cress seed (*Lepidium sativum*) gum and xanthan gum: Effect of refrigeration condition. Food Biosci. 2014;5:1–8.
28. Naji S, Razavi SM, Karazhiyan H. Effect of freezing on functional and textural attributes of cress seed gum and xanthan gum. Food Bioprocess Technol. 2013;6(5):1302–11.
29. Naji S, Razavi SMA, Karazhiyan H. Effect of thermal treatments on functional properties of cress seed (*Lepidium sativum*) and xanthan gums: a comparative study. Food Hydrocolloids. 2012;28(1):75–81. https://doi.org/10.1016/j.foodhyd.2011.11.012.

30. Niknam R, Ghanbarzadeh B, Ayaseh A, Rezagholi F. The effects of Plantago major seed gum on steady and dynamic oscillatory shear rheology of sunflower oil-in-water emulsions. J Texture Stud. 2018;49(5):536–47.
31. Ostrowska-Czubenko J, Pieróg M, Gierszewska-Drużyńska M. State of water in noncrosslinked and crosslinked hydrogel chitosan membranes–DSC studies. Prog Chemistry Appl Chitin Deriv. 2011;16:147–56.
32. Paramera EI, Konteles SJ, Karathanos VT. Stability and release properties of curcumin encapsulated in Saccharomyces cerevisiae, β-cyclodextrin and modified starch. Food chem. 2011;125(3):913–22.
33. Pham L, Truong MD, Nguyen TH, Le L, Nam ND, Bach LG, Tran NQ. A dual synergistic of curcumin and gelatin on thermal-responsive hydrogel based on Chitosan-P123 in wound healing application. Biomed Pharmacother. 2019;117: 109183.
34. Pilevaran M, Tavakolipour H, Naji-Tabasi S, Elhamirad AH. Development of mechanical and thermal properties of whey protein–xanthan gum hydrogel by incorporation of basil seed gum nanoparticles, salt, and acidic pH. J Sol-Gel Sci Technol. 2021;98(1):76–83.
35. Pongjanyakul T, Puttipipatkhachorn S. Xanthan–alginate composite gel beads: molecular interaction and in vitro characterization. Int J Pharm. 2007;331(1):61–71.
36. Rao KM, Mallikarjuna B, Krishna Rao K, Sudhakar K, Rao KC, Subha M. Synthesis and characterization of pH sensitive poly (hydroxy ethyl methacrylate-co-acrylamidoglycolic acid) based hydrogels for controlled release studies of 5-fluorouracil. Int J Polym Mater Polym Biomater. 2013;62(11):565–71.
37. Razavi SM, Naji-Tabasi S. Rheology and texture of cress seed gum. In: Karpushkin E, editor. Principles, applications and environmental impacts. New York: Nova Science Pub Inc; 2015.
38. Razmkhah S, Razavi SMA, Mohammadifar MA. Dilute solution, flow behavior, thixotropy and viscoelastic characterization of cress seed (Lepidium sativum) gum fractions. Food Hydrocolloids. 2017;63:404–13.
39. Reddy OS, Subha M, Jithendra T, Madhavi C, Rao KC. Curcumin encapsulated dual cross linked sodium alginate/montmorillonite polymeric composite beads for controlled drug delivery. J Pharm Anal. 2021;11(2):191–9.
40. Saeedi M, Morteza-Semnani K, Akbari J, Bazargani MH, Amin G. Evaluation of Ocimum basilicum L. seed mucilage as rate controlling matrix for sustained release of propranolol HCl. Pharm Biomed Res. 2015;1(1):18–25.
41. Segovia N, Pont M, Oliva N, Ramos V, Borrós S, Artzi N. Hydrogel doped with nanoparticles for local sustained release of siRNA in breast cancer. Adv Healthcare Mater. 2015;4(2):271–80.
42. Shahbazizadeh S, Naji-Tabasi S, Shahidi-Noghabi M, Pourfarzad A. Development of cress seed gum hydrogel and investigation of its potential application in the delivery of curcumin. J Sci Food Agric. 2021;101:6505–13.
43. Sivakumaran D, Maitland D, Hoare T. Injectable microgel-hydrogel composites for prolonged small-molecule drug delivery. Biomacromol. 2011;12(11):4112–20.
44. Sivakumaran D, Maitland D, Oszustowicz T, Hoare T. Tuning drug release from smart microgel–hydrogel composites via cross-linking. J Colloid Interface Sci. 2013;392:422–30.
45. Sonia T, Sharma CP. Chitosan and its derivatives for drug delivery perspective. Chitosan Biomaterials. 2011;I:23–53.
46. Szekalska M, Sosnowska K, Czajkowska-Kośnik A, Winnicka K. Calcium chloride modified alginate microparticles formulated by the spray drying process: a strategy to prolong the release of freely soluble drugs. Materials. 2018;11(9):1522.
47. Taktak F, Yildiz M, Sert H, Soykan C. A novel triple-responsive hydrogels based on 2-(dimethylamino) ethyl methacrylate by copolymerization with 2-(N-morpholino) ethyl methacrylate. J Macromolecular Sci A. 2015;52(1):39–46.
48. Tansaz S, Singh R, Cicha I, Boccaccini AR. Soy protein-based composite hydrogels: physico-chemical characterization and in vitro cytocompatibility. Polymers. 2018;10(10):1159.
49. Tapal A, Tiku PK. Complexation of curcumin with soy protein isolate and its implications on solubility and stability of curcumin. Food Chem. 2012;130(4):960–5.
50. Thongchai K, Chuysinuan P, Thanyacharoen T, Techasakul S, Ummartyotin S. Characterization, release, and antioxidant activity of caffeic acid-loaded collagen and chitosan hydrogel composites. J Market Res. 2020;9(3):6512–20.
51. Torres-Figueroa AV, Pérez-Martínez CJ, Castillo-Castro T, Bolado-Martínez E, Corella-Madueño MA, García-Alegría AM, Armenta-Villegas L. Composite Hydrogel of Poly (acrylamide) and starch as potential system for controlled release of amoxicillin and inhibition of bacterial growth. J Chem. 2020;2020:1.
52. Vigata M, Meinert C, Hutmacher DW, Bock N. Hydrogels as drug delivery systems: a review of current characterization and evaluation techniques. Pharmaceutics. 2020;12(12):1188.
53. Widjaja LK, Bora M, Chan PNPH, Lipik V, Wong TT, Venkatraman SS. Hyaluronic acid-based nanocomposite hydrogels for ocular drug delivery applications. J Biomed Mater Res Part A. 2014;102(9):3056–65.
54. Xiong, S. Q., Wang, Y., Zhu, J., Hu, Z. M., & Yu, J. R. (2016). Polydopamine nanoparticle for poly (N-isopropylacrylamide)-based nanocomposite hydrogel with good free-radical-scavenging property. *Materials Science Forum* (Vol. 848, pp. 94–98): Trans Tech Publ.
55. Ye Y, Hu X. A pH-sensitive injectable nanoparticle composite hydrogel for anticancer drug delivery. J Nanomaterials. 2016;2016:1.
56. Zeynali M, Naji-Tabasi S, Farahmandfar R. Investigation of basil (Ocimum bacilicum L.) seed gum properties as Cryoprotectant for Frozen Foods. Food Hydrocoll. 2019;90:305–12.
57. Zhao F, Yao D, Guo R, Deng L, Dong A, Zhang J. Composites of polymer hydrogels and nanoparticulate systems for biomedical and pharmaceutical applications. Nanomaterials. 2015;5(4):2054–130.
58. Zheng C, Huang Z. Microgel reinforced composite hydrogels with pH-responsive, self-healing properties. Colloids Surf A. 2015;468:327–32.

Publisher's Note
Springer Nature remains neutral with regard to jurisdictional claims in published maps and institutional affiliations.